Disturb or Stabilize? A Molecular Dynamics Study of the Effects of Resorcinolic Lipids on Phospholipid Bilayers

Magdalena E. Siwko,[†] Alex H. de Vries,[†] Alan E. Mark,[‡] Arkadiusz Kozubek,[§] and Siewert J. Marrink[†*]
[†]Department of Biophysical Chemistry, University of Groningen, Groningen Biomolecular Sciences and Biotechnology Institute, Groningen, The Netherlands; [‡]School of Molecular and Microbial Sciences, University of Queensland, the Institute for Molecular Biosciences, Brisbane, Australia; and [§]Department of Lipids and Liposomes, University of Wroclaw, Wroclaw, Poland

ABSTRACT Resorcinolic lipids, or resorcinols, are commonly found in plant membranes. They consist of a substituted benzene ring forming the hydrophilic lipid head, attached to an alkyl chain forming the hydrophobic tail. Experimental results show alternative effects of resorcinols on lipid membranes. Depending on whether they are added to lipid solutions before or after the formation of the liposomes, they either stabilize or destabilize these liposomes. Here we use atomistic molecular dynamics simulations to elucidate the molecular nature of this dual effect. Systems composed of either one of three resorcinol homologs, differing in the alkyl tail length, interacting with dimyristoylphosphatidylcholine lipid bilayers were studied. It is shown that resorcinols preincorporated into bilayers induce order within the lipid acyl chains, decrease the hydration of the lipid headgroups, and make the bilayers less permeable to water. In contrast, simulations in which the resorcinols are incorporated from the aqueous solution into a preformed phospholipid bilayer induce local disruption, leading to either transient pore formation or even complete rupture of the membrane. In line with the experimental data, our simulations thus demonstrate that resorcinols can either disturb or stabilize the membrane structure, and offer a detailed view of the underlying molecular mechanism.

INTRODUCTION

1,3-dihydroxy-5-*n*-alk(en)ylbenzenes, referred to alternatively as alkylo-resorcinolic lipids (ARs), resorcinols, or RES+tail length, are a group of naturally occurring compounds that are common components of biological membranes. The basic element, orcinol, consists of a benzene ring with two hydroxyl groups substituted at positions 1 and 3 and with the alkyl tail attached at position 5. The structures of orcinol and resorcinol are shown in Fig. 1. Natural orcinol derivatives differ in the alkyl tail and are classified according to a combination of tail length (11–29 carbons) and the degree of unsaturation (0–4 carbons). In nature, resorcinols usually occur as a mixture of several homologs.

ARs occur primarily in higher plants (e.g., *Anacardiaceae*, *Ginkoaceae*), but also in some lower plants (algae, mosses, fungi). Saturated homologs are found exclusively in specific strains of bacteria (*Azotobacter*, *Pseudomonas*). Resorcinolic lipids are not usually found in animal tissue but have been reported in the marine sponge. In particular, ARs are found in high concentration in the bran of certain cereals (wheat, oats, and rye). For many years, ARs were thought to be secondary metabolites and not to play a major role in cellular physiology. More recently, ARs have been shown to have a range of important biological functions and have attracted much attention in fields such as nutrition (1,2), agriculture (3,4), and medicine (5).

Resorcinols are amphiphilic due to the nonisoprenoid side chain attached to the dihydroxybenzene ring. Like many lipids, the phase behavior of ARs can be understood in terms of simple geometric concepts (6). Short tail ARs can be thought of as cone-shaped and have a tendency to form micellar type structures. The shape of ARs become more cylindrical with longer alkyl tails and lamellar structures become more favorable. Resorcinolic lipids have very low critical micelle concentrations in the range of 4.5–8.5 μM and are thus practically insoluble in water. The specific value depends on the homolog (tail length and degree of unsaturation). The preference of ARs for a hydrophobic environment is also reflected in the high octanol/water partition coefficient ($logP_{o/w} = 12$) (7).

Experimentally, resorcinolic lipids induce a range of structural changes in phospholipid membranes. Gubernator et al. showed that resorcinolic lipids can affect phospholipid membranes differently depending on the way they are added to the system (8). If added before phospholipid vesicles are formed, ARs showed a stabilizing effect on phospholipid bilayers. The membrane becomes more resistant to the permeation of small solutes, such as water, ions, and glucose (9–12), and vesicles are more resistant to osmotic stress (13). Kozubek et al., using electron spin resonance techniques, found that biological activity depends strongly on the structural characteristics of the specific homolog and that the inclusion of resorcinol leads to a shift in the gel-liquid crystalline phase transition of a DPPC bilayer to higher temperatures (14). In contrast, when added to a suspension of liposomes (i.e., when the vesicles are already formed), ARs increase the release of soluble markers from the liposomes (11,15). ARs can also lead to hemolysis of blood cells (10,12). This effect is significant at high concentrations (>15 mol %). At concentrations of 50 mol % and above, they also

Submitted September 16, 2008, and accepted for publication January 16, 2009.

*Correspondence: s.j.marrink@rug.nl

Editor: Reinhard Lipowsky.

0006-3495/09/04/3140/14 $2.00

doi: 10.1016/j.bpj.2009.01.040

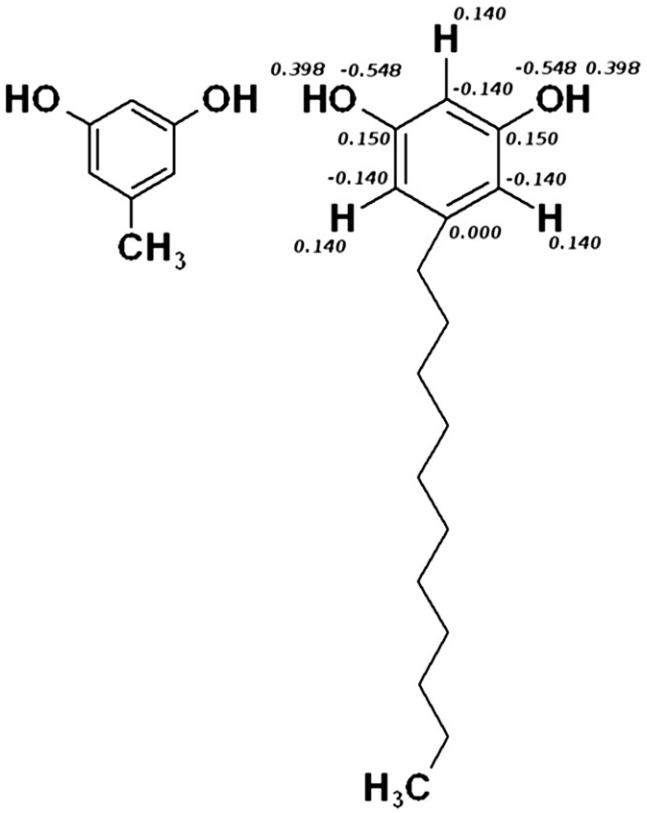

FIGURE 1 Structures of orcinol (*left*) and 1,3-dihydroxy-5-*n*-alkylbenzene, known as resorcinol (*right*). Partial charges of the dihydroxybenzene used in the simulations have been placed at the corresponding atoms.

have a fusiogenic effect on yeast protoplasts (16). Longer tails and more unsaturated bonds enhance the dual effect of resorcinols on biological membranes.

The range of biological activities of resorcinols makes them attractive for the pharmaceutical and nutrition industries. Resorcinols can be used as markers in the assessment of the nutritional value of cereal products (1) or as part of novel liposomal formulations for drug delivery (5,17). For example, unsaturated homologs may serve as protectants against free radicals that induce lipid oxidation (18,19). This is especially important in cardiovascular disease. Alternatively, since long tail resorcinols have a stabilizing effect on membranes similar to that of cholesterol, it has been proposed that cardanol, a resorcinol derivative containing only one hydroxyl group in the aromatic ring and 15 carbon atoms, could be more effective than cholesterol in stabilizing liposomes in certain drug formulations (20).

In this article, we describe molecular dynamics (MD) simulations of the interaction of resorcinols with dimyristoyl-phosphatidylcholine (DMPC) lipid bilayers, using an atomistic force field. Experimentally, resorcinols have only a minor effect on phospholipid membranes below a concentration of 15 mol %. Above a concentration of 50 mol %, lamellar structures are unstable. For this reason, simulations of three saturated resorcinolic derivatives were performed at a concentration of 30 mol %, close to that commonly used in experimental studies (8,21). The chosen homologs differ with respect to the length of the tail (11, 19, and 25 carbon atoms). First, the spontaneous aggregation of different mixtures is simulated to get an unbiased view of the preferred aggregation state of the DMPC/AR mixed systems. Subsequently we simulated preassembled bilayer systems, either with the resorcinols preincorporated or with the resorcinols initially dispersed randomly in the aqueous solution. Details of the simulations are given in the following section, followed by a presentation of the results and a discussion of the dual disturbing and stabilizing effects of resorcinols on phospholipid bilayers. A short conclusion ends the article.

METHODS

Simulation details

All MD simulations were performed using the GROMACS (Ver. 3.0.5) package (22). The parameters for the resorcinolic lipids were selected such that they were consistent with the parameters for PC lipids (23). The acyl chains were represented by united atoms (CH2, CH3). Polar hydrogens such as the hydrogens of the hydroxyl groups and those attached to the aromatic ring were treated explicitly. Within the benzene ring, 1–4 interactions were excluded, as is the standard practice within the GROMOS96 force field (24). The charges of the dihydroxy benzene ring (for details, see Fig. 1) were obtained from the electron density calculated at the semiempirical QM level with bond-charge corrections using the restrained electrostatic potential method (25). The simple point charge water model was used (26). Covalent bond lengths were constrained using the LINCS algorithm (27). Nonbonded interactions were computed using a twin-range cutoff. Within the short-range cutoff of 1.0 nm, van der Waals and Coulomb interactions were updated every step. Coulomb interactions within the long-range cutoff of 1.4 nm were updated every 40 fs (10 time steps) together with the neighbor-list. The temperature was controlled by weakly coupling the system to a heat bath at 323 K using a Berendsen thermostat (28) with a coupling time constant of 0.1 ps. The main components of the system (DMPC, resorcinols, water) were coupled independently to the heat bath. The pressure was maintained by coupling the system using a Berendsen barostat (28) to an external pressure bath at 1 bar with a coupling time constant of 1.0 ps and compressibility of 5.0×10^{-5} bar^{-1}. The coordinates were scaled anisotropically (x, y, and z directions were scaled independently) or semiisotropically (x and y directions were scaled together leaving the z direction independent) depending on the system. To correct for the truncation of the electrostatic interactions beyond the 1.4-nm long-range cutoff, a reaction-field correction (29) with a relative dielectric constant of 54 was used (30). The integration time step was 4 fs.

Systems

To investigate how resorcinolic lipids affect the properties of a phospholipid membrane, three different types of simulation were performed. The first involved the spontaneous aggregation of mixtures of ARs and DMPC in water. The second involved the simulation of equilibrated symmetric DMPC/AR bilayers. The third involved the simulation of the interaction of resorcinolic lipids placed in the aqueous phase next to a preformed DMPC bilayer. Three saturated resorcinol homologs were considered, RES11, RES19, and RES25, which differ in the length of the alkyl tail. The concentration of the ARs is (approximately) 30 mol % in all systems. Table 1 gives an overview of all simulations performed. For comparison, a previous simulation for a pure DMPC bilayer (31), is also included.

TABLE 1 Overview of all simulations performed

Label	N_{sim}	$N_{DMPC/AR}$	$N_{sol/lipid}$	t_{sim} (ns)
pureDMPC (31)	2	64/0	25	80, 80
aggRES11	2	64/22	30	40, 92
	1	64/21	27	40
aggRES19	2	64/28	29	40, 140
	1	64/21	29	100
aggRES25	2	64/21	34	60, 160
symmRES11	1	62/18	25	80
symmRES19	1	62/18	25	80
symmRES25	1	58/16	25	80
incrpRES11-s	3	64/28	35	75, 80, 170
incrpRES19-s	3	64/28	35	42, 55, 160
incrpRES25-s	3	64/28	35	30, 30, 170
incrpRES11-l	3	256/112	35	130, 316, 360
incrpRES19-l	3	256/112	49	160, 175, 240
incrpRES25-l	2	256/112	49	90, 120

Labels correspond to the type of the simulation and the homolog of the resorcinol. Systems with labels *agg-* and *pure-* correspond to the aggregation of mixed or pure systems, respectively. Labels *incrp-* correspond to the incorporation and the *symm-* correspond to the simulation of the preincorporated resorcinols into the DMPC bilayer. N_{sim} denotes the number of simulations performed; $N_{DMPC/AR}$ corresponds to the number of DMPC or AR in the system; $N_{sol/lipid}$ corresponds to the number of water molecules per lipid; t_{sim} corresponds to the time of the simulation.

Spontaneous aggregation of mixed DMPC/AR systems

The three systems (see Table 1) used to investigate the spontaneous aggregation of AR and DMPC were constructed according to the general procedure outlined below. One of four different conformations of a chosen component, i.e., ARs and DMPC was placed randomly within a cubic box of a given size using the GROMACS tool Genbox. After the required number of molecules had been placed in the simulation box, the box was filled with 30–35 waters per molecule (AR or DMPC). The initial configurations were then energy-minimized. An initial 20-ps simulation using a 1-fs time step and isotropic pressure coupling at 1 bar was performed to relax the configuration. Then the time step was increased to 4 fs, anisotropic pressure coupling was applied, and the systems were simulated until well equilibrated. Production runs were in the range of 15–150 ns, depending on the time required for the system to fully stabilize. For each resorcinolic homolog, simulations were repeated up to three times with different starting configurations.

Preincorporated DMPC/AR bilayers

To investigate the stabilizing effect of resorcinols on a biological membrane and how this depends on the length of an alkyl tail, three symmetric systems were studied. Each monolayer contained an identical number of DMPC and resorcinol molecules. Starting configurations were taken from the spontaneous aggregation simulations of DMPC and resorcinol described above. To make the system symmetric, any excess of lipids in a given monolayer were removed. This meant that the final composition differed slightly for each of the three homologs (see Table 1). The hydration level was decreased to 25 waters per lipid for reasons of computational efficiency. After energy minimization and a short equilibration period of 100 ps, all systems were simulated for 80 ns. To avoid the deformation of the box in one of the lateral directions, semiisotropic coupling, in which the box fluctuations in the x and y axes are coupled, was used.

Incorporation of ARs into preformed DMPC bilayers

The mechanism of incorporation of the resorcinolic lipids into a preformed phospholipid bilayer was studied using six different systems. The first three involved 64 DMPC and 28 resorcinol molecules solvated with 35 waters per lipid. These small systems are labeled incrpRes11-s, incrpRes19-s, and incrpRes25-s, respectively. To check whether the size of the box affected the mechanism of incorporation, two sets of simulation systems four times larger than the original one were also constructed. These systems consisted of 256 DMPC and 112 resorcinols with the same hydration as the original system (35 waters per DMPC or AR molecule). In the case of the long tail homologs (RES19, RES25) preliminary simulations showed the interaction of resorcinol micelles with their periodic images. For this reason, the level of hydration was increased to 49 waters per DMPC or AR molecule. The large systems are labeled incrpRes11-l, incrpRes19-l, and incrpRes25-l, respectively (see Table 1). The starting structures of the small systems were prepared using the pure DMPC bilayer (64 DMPC). All solvent was removed and 28 resorcinolic lipids were placed randomly in the space available. To accommodate all resorcinols and maintain a constant level of hydration, the size of the box was increased in the z direction by 2.5–9.0 nm. It was also checked that individual resorcinol molecules were not in direct contact with the surface of the membrane. If a resorcinol molecule was in direct contact with the membrane, it was removed and a new position was randomly chosen. This was done to avoid the rapid insertion of resorcinol molecules into the membrane. The larger systems were constructed by replicating the initial box in the x and y directions before solvating with either 35 or 49 water molecules per DMPC or AR molecule. An initial series of 10-ns simulations were performed. Only those cases in which all resorcinols approached the bilayer from one side were kept for further study. In those cases, the simulations were extended to between 80 ns and 360 ns. The details of the simulations performed are given in Table 1.

Analysis

The results from the simulations were analyzed in terms of a range of structural and dynamic properties at equilibrium, including the mass density distribution, order parameters, headgroup hydration, and flux of water through the membrane. The analysis was performed using standard GROMACS tools (32). In addition, visual inspection was used to characterize the nature of the intermediate states occurring during the incorporation of resorcinols into the bilayer.

Calculation of the order parameters

As a measure of the order within the DMPC/AR bilayer, deuterium order parameters, S_{CD}, which will be referred to simply as order parameters, were calculated for the DMPC acyl chains and for the alkyl tail of resorcinol homologs. Because there are no explicit H-atoms in the simulations, the order parameters were calculated from the positions of the C-atoms along the chain (33). The standard error for S_{CD} was obtained by considering the time averaged value $\langle S_{CD} \rangle$ for each of the 64 DMPC molecules independently.

Calculation of the mass density distribution

The lateral inhomogeneity of the system was analyzed by calculating the mass density distribution across the bilayer. The mass density distributions were calculated for DMPC, AR, and solvent molecules and for certain groups of atoms, namely, the carbonyl and phosphate groups of DMPC and hydroxyl groups of resorcinol. The distance (D_{P-P}) between the two peaks in the mass distribution profile of the DMPC phosphate groups was used to determine the thickness of the bilayer. Leaflets 1 and 2 were defined based on the z-position of the single trimethylamine group of DMPC relative to the center of the bilayer, with the membrane oriented in the x,y plane. Separate values for the lipids in leaflet 1 and 2 indicate the degree of asymmetry in the final configuration.

Characterization of the hydration level

The effect of resorcinolic lipids on the level of hydration of the phospholipid membrane was determined by calculating the number of water molecules bound to the lipids. This was achieved by analyzing the number of water-lipid hydrogen bonds and analyzing water-lipid radial distribution

functions. The number of hydrogen bonds was calculated between water molecules and specific groups of atoms of the phospholipid, such as the carbonyl group and the phosphate group. The number of hydrogen bonds formed between the hydroxyl groups of resorcinols and water reflects the differences between the resorcinol homologs. Hydrogen bonds were determined based on cutoffs for the angle donor-hydrogen-acceptor of 30° and the distance hydrogen-acceptor of 0.35 nm. The radial distribution functions $g(r)$ of water around the groups of atoms specified above provide information about the hydration of various parts of the headgroups of DMPC. Hydration numbers were determined by integrating the radial distribution function to the first minimum.

Estimation of the water flux

The resistance of the membranes to the passage of water was estimated by calculating the flux of water through the bilayer. A flux event was counted as successful once a water molecule passed the central region of the bilayer. The width of this region was taken as 1.0 nm. Flux events from the left to the right (L → R) and from the right to the left (R → L) side of the bilayer were distinguished. The trajectories were sampled with a frequency of 1/40 ps^{-1} for this analysis. Error estimates are calculated by subdividing the trajectory into parts of 20-ns length and collecting statistics over the unidirectional flux events taking place in that period of time.

RESULTS

Spontaneous aggregation of DMPC/AR systems

To predict the preferred aggregation state of the mixed lipid/resorcinol systems, three sets of simulations starting from a random spatial arrangement of all the components were performed. The results are summarized in Table 2. In all of these simulations, the lipids spontaneously aggregate into a bilayer. The process of aggregation for the RES19 homolog is illustrated in Fig. 2. Within 4 ns, the initially random mixture of phospholipid and resorcinol molecules in water (see Fig. 2 *a*) separated, with the hydrophobic tails becoming distinct from the aqueous phase (Fig. 2 *b*). Further rearrangements led to the formation of a bilayer structure with a transmembrane water pore. This metastable intermediate with the hydrophilic headgroups of a few lipids lining the pore (Fig. 2 *c*) collapses within 50–60 ns of the simulation. During the final stage, the bilayer relaxes to its equilibrium state (Fig. 2 *d*). In the system involving the RES11 homolog, a complete bilayer was formed within 20 ns. The pore was formed mainly by DMPC molecules. None of the RES11 molecules showed any particular preference for the pore. In contrast, almost 80% of the long tail homologs (RES19, RES25) stayed in the region of the pore. The most stable water pore was found in the system containing the RES25 homolog, which collapsed only after 80 ns. In the final state, the lipids were uniformly distributed laterally, i.e., no separation between the DMPC and AR molecules was observed within each monolayer. However, the

TABLE 2 A summary of the spontaneous aggregation simulations

		Total	Leaflet 1	Leaflet 2
Label		DMPC/AR	DMPC/AR	DMPC/AR
pureDMPC (31)	2	64/0	32/0	32/0
aggRES11	1	64/22	34/6	30/16
	2	64/22	32/9	32/13
	3	64/21	34/12	30/9
aggRES19	1	64/28	31/17	33/11
	2	64/21	29/8	35/13
	3	64/28	30/11	34/17
aggRES25	1	64/21	33/9	31/12
	2	64/21	30/9	34/12

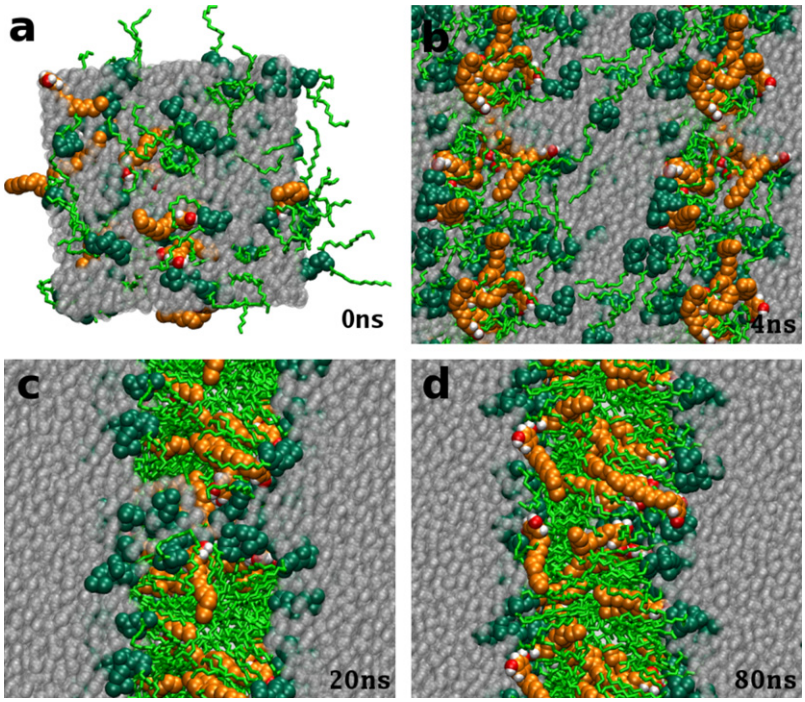

FIGURE 2 Snapshots of the spontaneous aggregation of a mixed DMPC/RES19 system. Snapshots were taken at 0 ns, 4 ns, 20 ns, and 80 ns of a 140-ns simulation. The initial simulation box with randomly distributed DMPC and RES19 molecules (*a*). A separation of the hydrophobic tails from the aqueous phase (*b*). The transmembrane water pore with a few lipids lining the pore (*c*). The final configuration of the equilibrated bilayer (*d*). The water is represented as light, semitransparent, diffusive shaded spheres; resorcinol molecules as light-shaded (*orange* in color version) spheres; and DMPC molecules are represented by dark-shaded (*green* in color version) spheres for headgroups, and sticks for the lipid tails.

TABLE 3 A comparison of structural properties of symmetric membranes with resorcinol preincorporated

System	$\langle S_{CD} \rangle$ DMPC/AR	D_{P-P} (nm)
pureDMPC (31)	0.162/–	3.3
symmRES11	0.21/0.19	3.65
symmRES19	0.22/0.12	3.8
symmRES25	0.22/0.10	3.7

$\langle S_{CD} \rangle$ is the order parameter averaged over all carbon atoms in the tails and averaged over both chains. D_{P-P} is a measure of membrane thickness, the distance between the maxima in the phosphate density distribution along the membrane normal. The standard errors are 0.02 for all values of $\langle S_{CD} \rangle$, and 0.1 for the membrane thickness.

distribution of lipids over the two leaflets was notably asymmetric (see Table 2). This phenomenon been observed before in spontaneous aggregation simulations of mixtures (34), and can be attributed to purely statistical effects. The average difference in the number of lipids between the two monolayers was eight molecules. It is important to note that the degree of asymmetry is larger for the resorcinolic lipids than for DMPC. The average asymmetry of DMPC was ~3 out of 64 molecules compared to 5 out of 28 molecules for resorcinol. The mixed DMPC/AR bilayers obtained by spontaneous aggregation are clearly not fully equilibrated. Further relaxation would require lipid flip flopping, a slow process not observable on the nanosecond timescale of the simulations. The asymmetric distribution of the components between the two monolayer leaflets makes further analysis problematic.

Preincorporated DMPC/AR bilayers

To study the interaction between resorcinolic and DMPC lipids in more detail, a set of preassembled bilayers was studied. These symmetric DMPC/AR bilayers, with the resorcinols preincorporated, were simulated for 80 ns. Equilibrium properties of these systems are shown in Tables 3–6, and are discussed in more detail below.

Tail order

Fig. 3 illustrates the order parameter profiles of the DMPC tails (Fig. 3 *a*) and of the three resorcinol homologs (Fig. 3 *b*) in the preincorporated DMPC/AR bilayers. The profiles are an average over both tails of the DMPC lipids or, in the case of resorcinols, over all resorcinol molecules of the specific homolog. In Fig. 3 *a*, the plain solid curve refers to the pure DMPC bilayer. The effect of the resorcinolic lipids on the order parameter profile of the DMPC lipid tails is to shift the profile to larger values. It can be seen from Fig. 3 *a* that, for DMPC, the inclusion of resorcinol into the system results in an increase in order of the segments closest to the headgroups and in the middle of the tail relative to that of the pure DMPC. Thus, whereas in pure DMPC the order parameter decreases almost linearly along the tail in the presence of resorcinols, there is a very short plateau, followed by a rapid decrease in order. In the case of resorcinols themselves, there is an apparent maximum in the order between positions 2 and 5 before a steep decrease in the order parameter (see Fig. 3 *b*). The difference in the values of the order parameters between the first and the last atom of the tail is larger for the resorcinols than for the tails of DMPC. This is most likely a result of resorcinols having only one alkyl tail and as a consequence more freedom to explore different conformations. A direct comparison of the $\langle S_{CD} \rangle$ between the homologs is difficult due to the different length of their tails. The average tail order of the DMPC lipids and resorcinol homologs in the membranes is given in Table 3. It is clear from Table 3 that the average order of the DMPC tails increases upon introduction of resorcinolic lipids in the membrane, from 0.16 to 0.22, and that the RES homolog does not influence the value strongly. In contrast, the average order of the alkyl chains of the resorcinol homologs appears to decrease with increasing length. As shown in Table 3, the RES11 homolog, perhaps somewhat surprisingly, has the highest order parameter: $\langle S_{CD} \rangle$ equals 0.19. Comparing just the average $\langle S_{CD} \rangle$ values is, however, misleading. The average value of the order parameter of the RES11 tail is

TABLE 4 Average number of hydrogen bonds formed between lipid and water and between lipids for pure DMPC and DMPC/AR systems

System	pureDMPC (31)	symmRes11	symmRes19	symmRes25
	per DMPC	per DMPC	per DMPC	per DMPC
DMPC-SOL	7.14 ± 0.02	6.68 ± 0.04	6.70 ± 0.03	6.72 ± 0.03
C=O-SOL	2.78 ± 0.01	2.45 ± 0.05	2.48 ± 0.02	2.47 ± 0.03
PO_4^--SOL	4.34 ± 0.01	4.23 ± 0.01	4.19 ± 0.01	4.24 ± 0.03
		per RES	per RES	per RES
OH-C=O		1.44 ± 0.03	1.35 ± 0.03	1.39 ± 0.01
OH-PO_4^-		0.42 ± 0.02	0.49 ± 0.05	0.41 ± 0.05
OH-SOL		1.08 ± 0.02	0.97 ± 0.05	1.12 ± 0.04

The table is divided in two parts. The upper part lists the average number of hydrogen bonds between DMPC and water (SOL) per DMPC lipid molecules, subdivided into contributions from carbonyl (C=O) and phosphate (PO_4^-) groups; the lower part lists the average number of hydrogen bonds between the hydroxyl groups (OH) of resorcinol and CO, PO_4^- of DMPC and water, respectively, per RES lipid molecule.

TABLE 5 Number of water molecules in the first hydration shell of the DMPC headgroup (PO_4^-, C=O)–water (OW), and of one of the AR hydroxyl groups (OH)

System	pureDMPC	symmRes11	symmRes19	symmRes25
PO_4^-	5.00	4.9	4.5	4.7
C=O	2.00	1.6	1.8	1.8
OH		0.8	0.8	0.8

high because the tail is short and the average is not dominated by values near zero at the end of the tail as in the case of the RES25 homolog. In fact, close to the headgroup, RES11 is less ordered than RES25. Away from the headgroup—carbons 5–9—the values of order parameters are the same for all homologs. Between carbons 14 and 17, the order parameters of RES25 fall almost to zero before rising again. When analyzing snapshots of the simulations of the RES19 and RES25 homologs, it is seen that the tails of these resorcinols adopt different types of configurations in the membrane, as illustrated in Fig. 4 for RES25. Three characteristic configurations can be identified:

1. A straight configuration in which the resorcinol penetrates into the opposite monolayer.
2. A bent configuration where the tails lies at the center of the bilayer.
3. A hairpin configuration where the tails fold back into the same monolayer.

Thus, the increase seen in the order parameter profile for the last six carbons of RES25 is due to the tail either folding back into the same leaflet or becoming embedded in the opposite leaflet.

Mass density distribution

Fig. 5 illustrates the mass density distribution of the DMPC bilayers. Fig. 5 *a* corresponds to the pure DMPC system. Fig. 5, *b–d*, corresponds to the bilayers in which RES11, RES19, and RES25 homologs have been preincorporated, respectively. The distributions of the DMPC, resorcinols, water, carbonyl groups (CO), phosphate groups (PO_4^-), and hydroxyl groups of resorcinols (OH) are plotted. The distribution of the OH groups correlates closely with the distribution of the carbonyl groups (*light-shaded areas*). This implies that the dihydroxybenzene rings have a high affinity for the region of the glycerol of the DMPC (see also Fig. 4). The distribution of the resorcinol molecules (*solid light-shaded area*) changes with the length of the tails (Fig. 5, *b–d*). The characteristic peak at the center of the bilayer represents the accumulation of the tails of the resorcinols. The longer the tail, the higher the peak. At the same time, the density of DMPC at the center of the bilayer decreases. The maximum drop is reached when the RES25 homolog is present with the density of DMPC dropping to 250 kg/m^3 (see Fig. 5 *d*). The accumulation of the tails of the resorcinols increases the thickness of the bilayer, as judged from the phosphate-phosphate peak distance, which is reported in Table 3. The smallest effect is observed for the RES11 homolog, the thickness increasing from 3.3 nm to 3.65 nm while the RES19 homolog increases the thickness to 3.8 nm. Surprisingly, in the case of the symmRES25 system, the thickness is 0.1-nm less than in the symmRES19

TABLE 6 Total number of water molecules permeating through pure DMPC and DMPC/AR bilayers, and permeability coefficient of the membranes for water

System	Flux events		Permeability
	L → R	R → L	P (cm s^{-1})
pureDMPC	12	7	0.020 ± 0.005
symmRES11	4	6	0.009 ± 0.003
symmRES19	2	5	0.007 ± 0.002
symmRES25	5	3	0.008 ± 0.003

L corresponds to the water that enters the membrane from the left side of the bilayer, *R* from the right side.

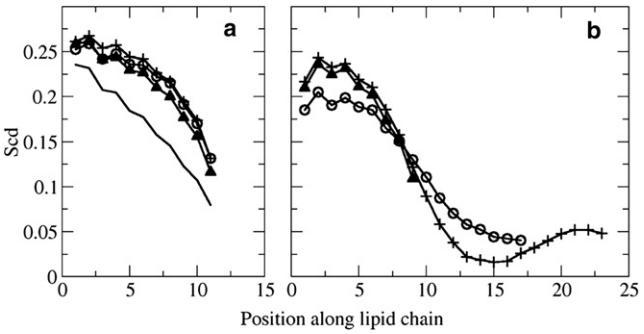

FIGURE 3 Deuterium order parameters profiles of the acyl chains of the DMPC (*a*) and of the resorcinol homologs (*b*). (*Solid line*) Order parameter profile of the pure DMPC; (*solid triangles*) RES11; (*open circles*) RES19; and (*crosses*) RES25.

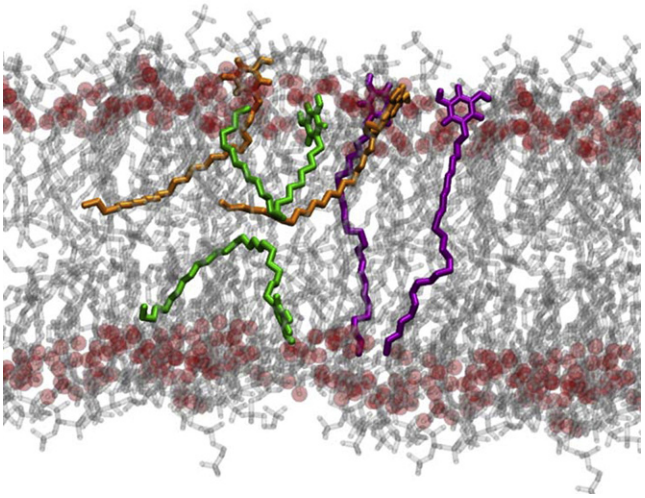

FIGURE 4 Possible configurations of resorcinolic tails in the membrane: penetration into opposite monolayer, accumulation in the center of the bilayer or back-folding. The oxygens (*darker spheres*) of the carbonyl groups have been emphasized to show that the dihydroxybenzene rings of resorcinols bind in this region. For clarity, the water has been removed.

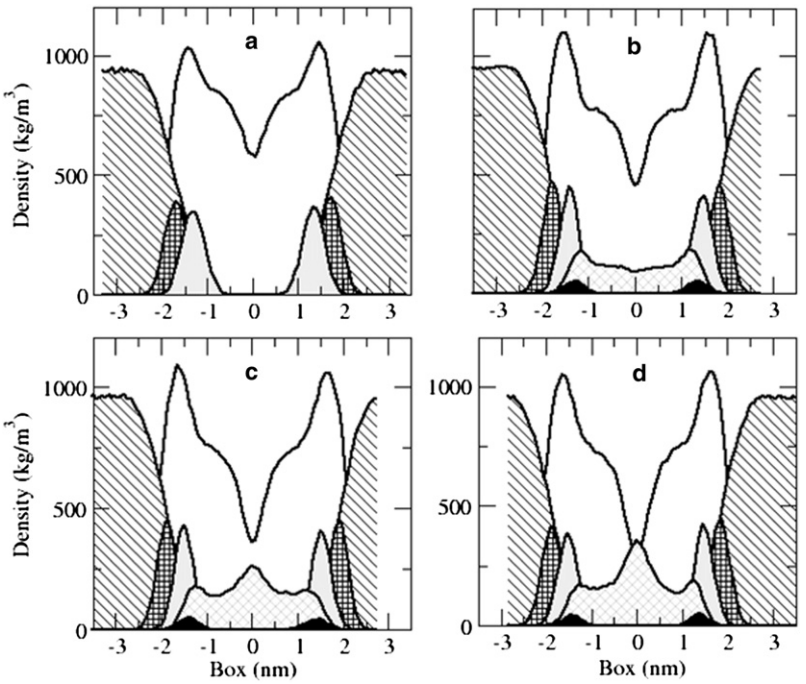

FIGURE 5 Mass density distribution of the DMPC bilayer along the z axis (normal to the bilayer). The distribution of the pure DMPC bilayer and its components (*a*). In *b–d*, the systems with the RES11, RES19, and RES25, respectively, are presented. The DMPC lipids (*unshaded area below the curve*), resorcinolic lipids (*solid light-shaded area*), water (*striped area*), carbonyl groups (*dotted shaded areas*), phosphate groups (*checkered areas*), and hydroxyl groups of resorcinols (*solid areas*) are shown separately.

system, even though the tails of this homolog are six carbons longer than that of the RES19 homolog. The reason for this apparent discrepancy is found in the increased backfolding of the tails of the longer homolog. In the systems containing resorcinols, the distribution of the phosphate groups and carbonyl groups is also narrower in comparison with the pure DMPC system. The distribution of water (*striped areas*) also changes. In the presence of the resorcinols, water penetrates less deeply into the interface, leaving the carbonyl groups less hydrated (this is not visible in Fig. 5 but will become clear from the analysis below).

Hydration properties

The number of hydrogen bonds between the phospholipids, resorcinols and water is given in Table 4. The total number of hydrogen bonds formed between DMPC and water in the pure DMPC system is ~7.1 per DMPC molecule. After adding resorcinol, this number decreases to 6.7 per DMPC. The number of hydrogen bonds between DMPC and water in the presence of various resorcinolic homologs is the same. The number of hydrogen bonds between the particular groups (i.e., phosphate groups, carbonyl groups) of the DMPC and water reflects the contribution of these groups to the binding of water and the change in the penetration of water after the addition of the resorcinols (see Table 4). The high affinity of resorcinolic OH groups for the ester oxygens of the lipid carbonyl groups affects the interaction of the carbonyl groups with water more than that of the phosphate groups. In the pure DMPC system, the carbonyl groups (CO) formed 2.8 bonds with water per DMPC, while in the mixed systems this number changes to 2.5 bonds per DMPC. The hydration of the phosphate groups is reduced only slightly, from 4.3 to 4.2 bonds per DMPC lipid. These differences are statistically significant, as the estimated error is <0.05. On average, the resorcinolic lipids form ~1.0 hydrogen bonds with water and ~1.8 with DMPC per AR molecule. The loss of hydrogen bonds between CO–SOL is more than compensated for by the increase of the bonds OH–CO by 1.4, and by OH–PO_4^- by 0.3–0.5 bonds per AR molecule.

Another measure of the numbers of water molecules bound to a particular group is the radial distribution function $g(r)$. The results of this analysis are presented in Table 5. In the pure DMPC system, five water molecules are present in the first hydration shell of the phosphate groups of the DMPC and two in the first hydration shell of the carbonyl groups. The hydration of the carbonyl groups reflects the penetration of the solvent into the membrane. In the presence of RES11, the number of waters bound to the DMPC is reduced by ~20%. Of all homologs, the short homolog (RES11) has the strongest effect on the penetration of water at the carbonyl level, but the weakest on the phosphate groups. The size of the hydration shell of the resorcinol molecules is the same for all three homologs.

Permeation of water through the bilayer

Table 6 illustrates the unidirectional flux of water molecules through an equilibrated bilayer with or without resorcinols. (Note that there is no net flux expected, as there is no driving force. The differences observed between the left-to-right and right-to-left fluxes reflect the stochastic nature of the permeation process.) The largest total number of permeation events is observed (19 waters over a period of 80 ns) for the pure DMPC system. For the systems with resorcinols, the flux

decreases significantly. The largest number of permeation events is observed with the RES11 homolog (10 waters over a period of 80 ns), compared to seven for RES19, and eight for RES25. The differences between homologs are, however, within the estimated error and therefore not significant. It is interesting to compare the flux obtained for pure DMPC to the permeation rate predicted previously by nonequilibrium MD simulations (35). The permeability coefficient can be obtained from the flux events reported in Table 6, by dividing the number of observed flux events per unit of time by the effective driving concentration and multiplying by the area. The effective driving concentration for the unidirectional flux is simply the bulk concentration of water (55 mol/Liter). The area is the lateral area of the DMPC bilayer (20 nm^2). Calculation leads to a resulting permeability coefficient of 0.02 cm s^{-1}, similar to that estimated from the nonequilibrium simulations (0.07 cm s^{-1} at 350 K) (35). Given the difference in system details, the agreement is good. Experimental permeability coefficients for water across lipid bilayers are also ~10^{-3}–10^{-2} cm s^{-1}.

Incorporation of resorcinolic lipids into preformed DMPC bilayers

The question of whether the effect of postincorporation is different from that of preincorporation on the properties of a membrane is addressed next. The process of incorporation of the three resorcinol homologs into a preformed DMPC bilayer was studied using two different system sizes (see Table 1). In the starting configuration, the resorcinols were randomly distributed in the aqueous phase. In the next sections we first describe the final state of the system. Then the details of the incorporation pathways are discussed, followed by an analysis of the structural characteristics of the membranes after the incorporation process.

Phase changes upon incorporation

The final phases that were obtained after the incorporation of the resorcinols differed between the homologs and between the small and large systems. Three alternative final phases could be distinguished:

1. A lamellar, liquid-crystalline phase (L_α).
2. A hexagonal phase (H_I).
3. A lamellar phase with a gel phase domain ($L_\alpha + L_\beta$).

In the incrpRES11-s and incrpRES11-l systems (small and large, respectively), the membrane adopted the L_α phase. In the case of incrpRES19-s and incrpRES19-l, the behavior differed between the small and large systems. The small systems eventually adopted the L_α phase in all three trials. For the large systems, the L_α phase was formed in only one case. The other simulations led to the formation of the H_I phase. In the incrpRES25-l system, the resorcinolic lipids formed a gel-phase domain within the membrane ($L_\alpha + L_\beta$). The simulations of the incrpRES25-s system were not continued because the micelle formed by the resorcinol molecules began to interact with its periodic image. The same problem was observed in the incrpRES25-l system at low levels of hydration.

Two pathways of incorporation

Fig. 6 presents a schematic diagram of the various intermediates observed during the process of incorporation. The associated time constants are listed in Table 7. The incorporation of the resorcinolic lipids into the DMPC bilayer occurred via either of two major pathways. Pathway I involved a direct incorporation of the resorcinols into one monolayer of the bilayer, whereas, in pathway II, the system passed through an intermediate state in which a water pore was formed in the bilayer (denoted L_α^P). The final phase of the systems that passed through pathway I was always lamellar (L_α), although in the case of incrpRES25-l system, a gel-phase domain coexisting with a liquid domain was formed ($L_\alpha + L_\beta$). The pore-forming pathway II finished in either the lamellar (L_α) or the hexagonal phase (H_I). For small systems of the RES11 and RES19 homolog, pathway I was identified in two simulations, and pathway II only in one simulation. The large RES11 and RES19 systems all followed pathway II, but the lamellar phase was formed only in one of the three trials. In the other two, the bilayer was solubilized and the nonlamellar hexagonal phase structure (H_I) was formed.

As shown in Fig. 6, the first three intermediates are common for both pathways. Initially, resorcinolic lipids were distributed randomly in the water phase ($L_\alpha + R$). The resorcinols rapidly aggregated, forming a micellar structure ($L_\alpha + M$). The time t_1 of the micelle formation was ~1–2 ns for the small systems and 3–6 ns for the large systems. This micellar aggregate gradually migrated to the DMPC bilayer, where it interacted progressively with the surface of the bilayer. The micelle-bound state is denoted L_α^M. The time required for the micelle to migrate to the surface is

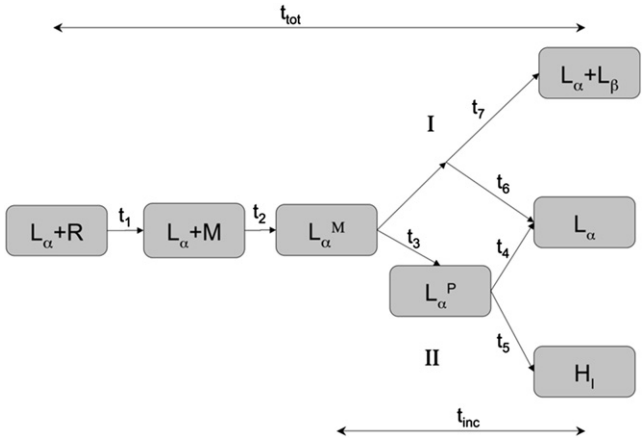

FIGURE 6 Diagram showing the evolution of the systems according to the two pathways (I and II). A detailed description of the diagram can be found in the text.

TABLE 7 Intermediate stages and the corresponding times of transitions (t_1–t_7) presented in Fig. 6

System	Pathway	$L_\alpha + M$	$L_\alpha{}^M$	$L_\alpha{}^P$	L_α	H_I	L_α	$L_\alpha + L_\beta$			
Time [ns]		t_1	t_2	t_3	t_4	t_5	t_6	t_7	t_{inc}	t_{tot}	t_{sim}
incrpRES11-s	I	2	10	—	—	—	47	—	47	59	170
incrpRES11-s	I	1	26	—	—	—	50	—	50	77	80
incrpRES11-s	II	1	10	10	22	—	—	—	32	43	75
incrpRES11-l	II	4	1	220	100	—	—	—	320	325	340
incrpRES11-l	II	1	1	316	—	—	—	—	—	—	318
incrpRES19-s	I	1	9	—	—	—	30	—	30	40	60
incrpRES19-s	I	1	8	—	—	—	33	—	33	42	42
incrpRES19-s	II	1	4	45	45	—	—	—	90	95	160
incrpRES19-l	II	2	8	14	—	—	54	—	68	78	175
incrpRES19-l	II	3	10	77	—	70	—	—	147	160	160
incrpRES19-l	II	3	4	130	—	35	—	—	165	172	240
incrpRES25-l	I	6	4	—	—	—	—	40	40	50	80
incrpRES25-l	I	6	4	—	—	—	—	30	30	40	90

The term t_{inc} corresponds to the total time of the insertion of the micelle into the bilayer, t_{tot} is the total time of the process of incorporation, and t_{sim} is the length of simulation.

indicated by time t_2, which is in the range of 1–26 ns. While the micelle stayed on the surface of the bilayer, the interactions between the resorcinol and DMPC increased. The phospholipids from the closest leaflet were forced to the center of the membrane, causing a strong deformation of the bilayer. The pathway that the system subsequently followed was influenced by the structure of the micelle. If the micelle formed by the resorcinols during the process of incorporation remained compact, an intermediate state with a water pore was favored (L_α^P). The phospholipids gradually surrounded the micelle, which was eventually fully incorporated within the closest leaflet (pathway II). Time t_3 reflects the time required to form the water pore once the micelle has absorbed into the membrane, and was found to vary between 10 and >300 ns. Times t_4 and t_5 indicate how long the water pore remained stable, either before closing (t_4) or until rupture (t_5). Pores remained stable on timescales between 20 and 100 ns. Alternatively, if the micelle did not become surrounded by phospholipids, but instead lost its integrity, resorcinols formed a layer on the surface of the membrane and insertion occurred without the formation of a pore (pathway I). In this case, a full disruption of the bilayer did not occur. Only one leaflet was disordered and resorcinols were inserted into that leaflet. This insertion occurred by the progressive incorporation of single lipids. Times t_6 and t_7 measure the complete insertion by pathway I by ~30–50 ns. The times associated with these successive stages suggest that if the pore is formed, the process of incorporation takes significantly longer (see t_{inc}, t_{tot}). After the complete incorporation of the resorcinols, the simulations were continued for at least 30 ns. However, none of the systems reached an equilibrium state during this time, mainly due to limitations in the rate of flip-flops between the two monolayers. In Fig. 7, pathway II is illustrated leading to a lamellar phase. The major intermediates during the incorporation of the RES19 homolog into a large DMPC bilayer are depicted.

Nonlamellar phase formation

Only for one system was complete disruption of the lamellar structure observed. The incrpRES19-l system formed a nonlamellar H_I structure, illustrated in Fig. 8. Initially, the resorcinolic micelle passed through a pore intermediate. Due to the strong interactions between the dihydroxybenzenes and choline groups, the micelle at the surface of the bilayer remained intact (Fig. 8 *b*). This prevented the insertion of the alkyl tails of resorcinols into the membrane. The whole micelle became gradually surrounded by phospholipids and was finally enclosed by the monolayer (Fig. 8, *c* and *d*), leading to the development of extreme curvature and overall distortion of the bilayer structure. Disruption of the bilayer was subsequently triggered by the formation of a water pore, coalescing with its periodic image in one of the lateral dimensions (Fig. 8 *e*). This led to the formation of tube-shape micelles stacked on top of each other (Fig. 8 *f*). This structure has the same topology as the hexagonal phase.

Gel phase domain formation

As noted above, the RES25 homolog formed a gel phase domain within the DMPC membrane ($L_\alpha + L_\beta$). The incorporation of the resorcinols in the incrpRES25-l system followed pathway I: formation of the micelle, migration to the bilayer, and gradual dissolution of the micelle inside the bilayer. However, due to the long tails of the RES25 homolog the aggregate remained compact and inserted as a single unit, as shown in Fig. 9. Within the bilayer, the resorcinols formed a domain where the tails of resorcinols gradually became more ordered, forming a gel phase. Interestingly, the part of the tail that extended beyond that of DMPC tails remained in the liquid-crystalline phase. Approximately the first 16 out of 25 carbons of the resorcinol tail became ordered. A few resorcinols, which did not incorporate into the gel phase domain, mixed freely with the phospholipids and remained disordered. The process of

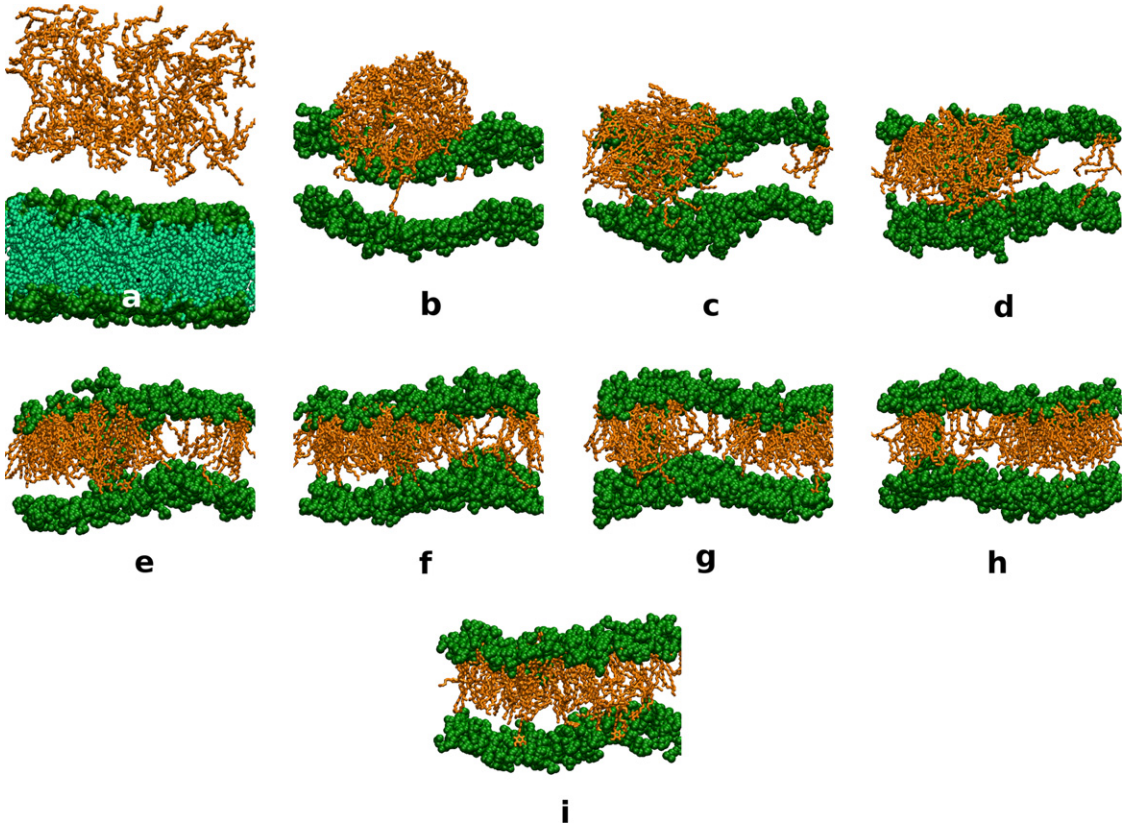

FIGURE 7 The incorporation of RES19 into a DMPC membrane. For clarity, tails of phospholipids were removed in snapshots *b–i* in a large system (RES19:DMPC 112:256). Snapshots were taken every 20 ns. The resorcinolic micelle forms from a random dispersion (*a*) and interacts with the surface of the bilayer (*b*). Increasing interactions of the resorcinols with the closest leaflet forced the phospholipids into the center of the bilayer (*c* and *d*). Consequently, the membrane lost its continuity. First the leaflet exposed to the resorcinols ruptured and later the second leaflet as well. A transient pore, through which water could diffuse, was formed (*d* and *e*). Resorcinol molecules then began inserting into the bilayer (*e–i*). This insertion occurred by the absorption of the whole aggregate. While the water pore existed, DMPC or AR molecules were able to diffuse into the center of the pore or even into the opposite monolayer. Lipids that moved to the center of the pore maintained the interaction of their headgroups with the water, thus stabilizing the pore.

incorporation of the RES25 homolog required ~70 ns of simulation (time t_7). After all resorcinols were in the bilayer, the simulation was continued for another 30 or 50 ns. Within this time, the phase separation remained.

Incorporation leads to large asymmetry within the membrane

The asymmetric incorporation of resorcinols into the DMPC bilayer leads to strongly asymmetric membrane properties. Fig. 10 illustrates the asymmetry in order parameter profiles of the tails of the DMPC in the two leaflets after the insertion of the resorcinols. The upper curve corresponds to the order parameter profile of tails in the monolayer enriched with RES11 and the lower curve corresponds to that of the monolayer with only one resorcinol molecule. The excess of DMPC and AR molecules in the one monolayer led to an increase in packing density. This was reflected in the order parameters of the tails of the DMPC in this monolayer. As can be seen in Fig. 10, the degree of order in the monolayer without RES11 decreases almost linearly along the alkyl tail and is much lower than the monolayer with more RES11. In the profile corresponding to the monolayer containing RES11, the largest increase in the order parameters is in the central segments of the alkyl tail. The shape of the profile is similar to the profiles of the preincorporated symmetrical systems (see Fig. 3).

The membrane asymmetry after incorporation of resorcinols is further reflected by the nonhomogeneous mass distribution. Fig. 11 compares the mass density distributions of the main components of the DMPC/RES11 system (at the initial and at the intermediate pore-forming stage) and the distribution of the pure DMPC bilayer (*dashed lines* in the figure). Although the presence of resorcinol increased the order of the alkyl tails, the thickness of the bilayer did not change (*overlapping dashed* and *solid lines*). Only the shape of the distribution of the DMPC lipids in the monolayer where the resorcinols were inserted changed. Resorcinols clearly accumulate in one monolayer only. Their hydroxyl groups reside at the level of the glycerol of the DMPC similar to the distribution in the preincorporated simulations (see Fig. 5).

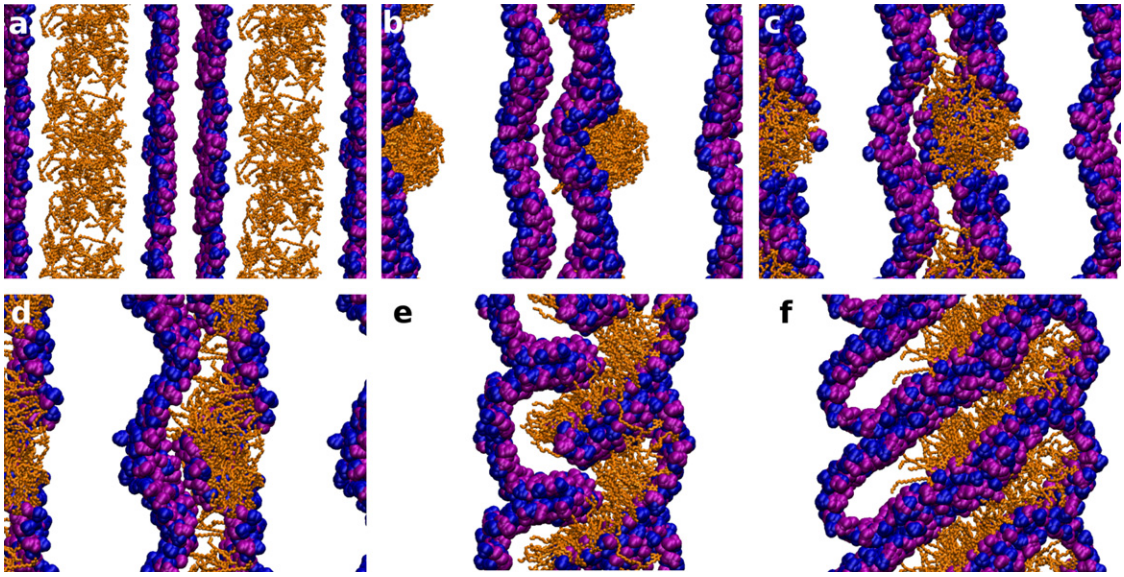

FIGURE 8 Snapshots illustrating the formation of a nonlamellar phase in the system including the RES19 homolog. Randomly distributed resorcinols (*a*) aggregate, forming an intact micelle (*b*). The strong affinity of resorcinols for the bilayer effects its disruption (*c* and *d*). This disruption leads to the formation of a water pore in the bilayer and a transition into a nonlamellar structure (*e* and *f*). For clarity, the phospholipid tails and solvent are removed. Light-shaded (*orange* in color version) lines represent resorcinolic lipids and dark-shaded (*blue-pink* in color version) spheres the headgroups of DMPC.

DISCUSSION

Resorcinols prefer a lamellar phase

To determine the preferred aggregation state of the resorcinolic lipids used in our studies, a series of spontaneous aggregation simulations were performed. The method of spontaneous aggregation provides an unbiased way to assess the preferred phase of the system. In each of the DMPC/AR systems, a bilayer was observed to form via an intermediate metastable state characterized by a water pore across the bilayer. These observations are in line with the mechanism of the bilayer formation proposed earlier by Marrink et al. (36) for DPPC lipids, and seen also in the aggregation of mixed PC/PE lipids (34) and pure DMPC (31). From our simulations, it can be concluded that the preferred aggregation state of mixtures of DMPC lipids and resorcinols is also lamellar. Additional simulations (not shown) reveal that the aggregation state of pure resorcinols at a comparable hydration level of 25–30 waters per molecule is also lamellar. Interestingly, the long tail (RES19 and RES25) homologs in the pure resorcinolic systems form a gel phase at physiological temperatures in agreement with experimental data (37,38). In mixtures, their behavior is rather different. The DMPC bilayers with preincorporated RES19 or RES25 remain homogeneously mixed in the liquid-crystalline phase. It cannot be excluded, however, that phase separation into a fluid DMPC-enriched and

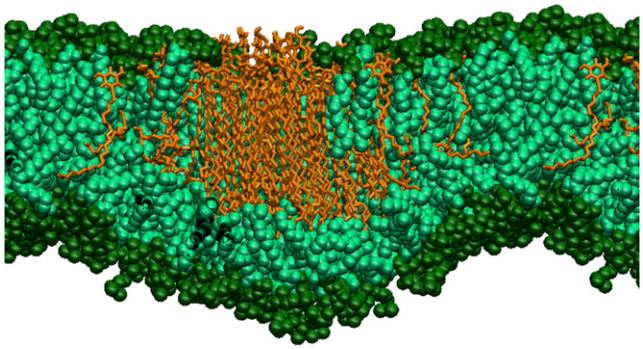

FIGURE 9 The gel domain formed by the RES25 homolog after incorporation in the DMPC bilayer. Resorcinols are represented as sticks, DMPC headgroups and their tails as spheres. The long tails of resorcinols are clearly ordered, especially the first part of the alkyl tail.

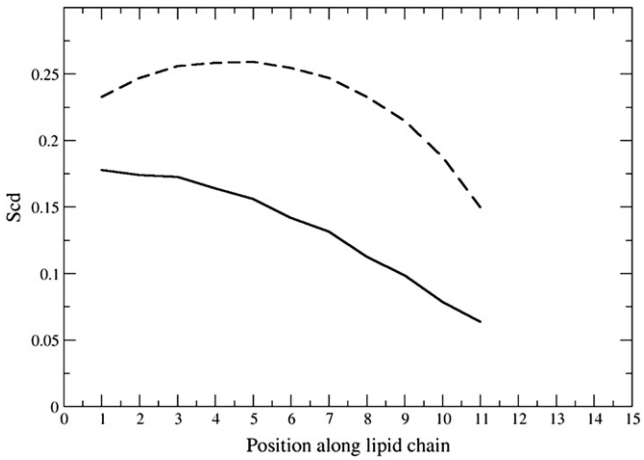

FIGURE 10 Deuterium order parameter profiles of DMPC lipid tails after asymmetric incorporation of the RES11 homolog. (*Solid line*) Leaflet with only one resorcinol. (*Dashed line*) Leaflet enriched with 28 resorcinol molecules.

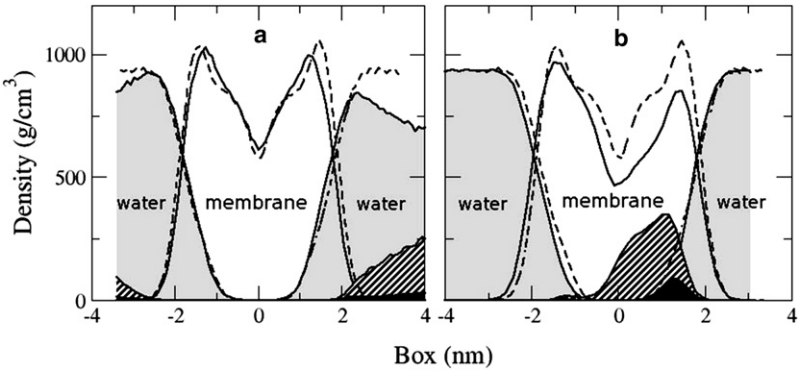

FIGURE 11 An illustration of the mass density distribution of the components in the mixed DMPC/RES11 bilayer of the incrpRES11-s system that followed pathway II, before the incorporation of resorcinols into DMPC membrane (*a*) and at the later stage where resorcinols are incorporated and a water pore is present (*b*). The striped area reflects the distribution of resorcinolic lipids, shaded fields correspond to the distribution of water, and solid areas represent hydroxyl groups of resorcinols. For comparison, the distribution of pure bilayer (DMPC and water) is represented by dashed lines.

a resorcinol-enriched gel domain might take place on longer timescales. In the case of the RES25 homolog, a gel phase domain is observed to be stable on the timescale of the simulation when incorporated as a micelle from the aqueous solution. Which of these two states is the true equilibrium state is not clear.

Cholesterol-like condensing effect of preincorporated resorcinols

A major question we aimed to address was how resorcinolic lipids affect the properties of the phospholipid membrane. The MD simulations show that the presence of resorcinolic lipids in the membrane strongly increases the degree of order in the membrane. This follows from the significant increase of the order parameter of the alkyl tails of DMPC (see Fig. 3 and Table 3). The values of the DMPC order parameters between homologs are comparable, suggesting that the ordering effect originates mainly from the presence of the resorcinolic headgroups. The increase in thickness, however, shows a clear dependence on the homolog. Especially in the case of RES25, the tail occupies space in between the monolayers, pushing them apart. Significant kinking and folding back of the tails in the case of RES25 is also observed (see Fig. 4). This packing effect of resorcinols is similar to the effect of cholesterol on membranes (14). By placing a rigid structure between the alkyl tails, cholesterol promotes the condensation of the tails and, at high concentration, induces a phase separation into a cholesterol-enriched liquid-ordered phase and a cholesterol-depleted liquid-crystalline phase (39,40). Although the structure of resorcinols is different from cholesterol, it has been claimed that the long tail homologs could induce the formation of separate resorcinol rich domains via a similar mechanism (41). The poor mixing of the RES25 homolog observed in our simulations, together with clear evidence of a cholesterol-like condensing effect, support this idea.

As a result of the condensation effect, the number of water molecules found around the carbonyl groups of DMPC decreases in the presence of resorcinol. The hydrogen bonds of DMPC with water are replaced in part by hydroxyl groups of resorcinol. In addition, water forms H-bonds with the resorcinolic headgroups. The most significant difference is observed between the pure DMPC system and the systems enriched with resorcinols. In this case, ~6% of hydrogen bonds were replaced by interactions with resorcinols. No preference for any specific homolog was observed (see Table 4), in agreement with the other results. Both the preincorporation and the incorporation simulations show that the dihydroxybenzene groups prefer to bind to the ester groups of the phospholipids. The length of the tail does not appear to influence the position of the resorcinol molecules. Due to the strong interactions between the hydroxyl groups of resorcinol and the glycerol oxygens, the membrane becomes dehydrated, limiting the penetration of water. The decreased hydration of the membrane is in agreement with experimental measurements of the kinetics of water in the headgroup region (42) and FT-IR experiments (43–45). In line with the decreased level of hydration, the number of water flux events is significantly decreased in the bilayers enriched in resorcinols compared to those in a pure DMPC bilayer. Again, this effect does not appear to depend strongly on the length of the tail.

Incorporation leads to leakiness

In strong contrast to the behavior of premixed DMPC/AR systems, the incorporation of resorcinols from the aqueous solution may lead to leakage of the membranes. After binding of the resorcinol micelle to the bilayer, a transient water pore may form which either collapses or leads to rupture of the bilayer. These results are in line with the experimental data where, after addition of the resorcinolic lipids into a suspension of DPPC liposomes, leakage of the liposomes is observed (11,12,21). The extreme consequence of the leakage is the transition to nonlamellar structures (43) or lysis of the membrane (10). The simulations show that the binding of the resorcinol to the lipid headgroup is a critical moment, which determines whether the system will evolve to local membrane rupture (i.e., pathway II) or smooth resorcinol insertion (i.e., pathway I). Due to the limited set of simulations performed, it is not possible to conclude which pathway is preferred by the specific resorcinols investigated. Both mechanisms are observed for the

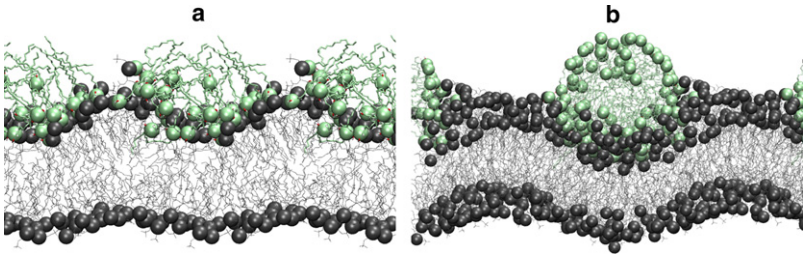

FIGURE 12 An illustration of the conditions under which the distribution of the resorcinols on the surface of the bilayer did not favor a pore formation (*a*) and the intact micelle, which creates sufficient stress to lead to the formation of the water pore (*b*).

same system, indicating that the direction along which the system evolves is governed by stochastic factors. Nevertheless, two important conditions must be fulfilled for poration to be observed: a strong deformation of the bilayer and a compact structure of the resorcinol aggregate, as illustrated in Fig. 12. A strong deformation in this context means that the structure of the monolayer is disrupted and the lipids start to surround the micelle. A compact micellar structure is characterized by a micelle that retains its spherical shape upon binding. Both conditions are likely coupled, i.e., a compact micelle triggers a strong deformation of the lipid bilayer and vice versa. The reason for pore formation is presumably the large stress created by an intact micelle absorbed onto one of the leaflets. The incorporation of the resorcinol means that there is almost a doubling of the number of molecules within this leaflet. This local stress induces the other monolayer to rupture. This is similar to what recently has been observed in simulations of pore formation by antimicrobial peptides (46,47), by dendrimers (48), and by surfactants (49). Despite the variety in chemical details of the adsorbing molecules, the underlying mechanisms of pore formation may have basic features in common.

CONCLUSION

In response to the question posed in the title of this article, we conclude that resorcinolic lipids have a dual effect on lipid membranes, i.e., they can both disturb and stabilize lipid membranes. Stabilization is observed when resorcinol is preincorporated into the membrane, in which case they increase the order of the lipid tails. As a consequence, the membrane thickens, the interface dehydrates, and the membrane becomes less permeable to water. In this regard, the effect of resorcinols is not dissimilar to the condensing effect of cholesterol. The disturbing effect takes place when the resorcinols are incorporated from the aqueous solution. In that case, an increase in leakiness is observed, caused by formation of transient water pores. Extrapolating to macroscopic systems, our results explain the experimentally observed transient leakage of liposomes due to the incorporation of resorcinols.

REFERENCES

1. Linko, A. M., K. S. Juntunen, H. M. Mykkanen, and H. Adlercreutz. 2005. Whole-grain rye bread consumption by women correlates with plasma alkyl resorcinols and increases their concentration compared with low-fiber wheat bread. *J. Nutr.* 135:580–583.
2. Ross, A. B., A. Kamal-Eldin, and P. Aman. 2004. Dietary alkyl resorcinols: absorption, bioactivities, and possible use as biomarkers of whole-grain wheat- and rye-rich foods. *Nutr. Rev.* 62:81–95.
3. Kozubek, A., R. Żarnowski, M. Stasiuk, and J. Gubernator. 2001. Natural amphiphilic phenols as biofungicides. *Cell. Mol. Biol. Lett.* 6:351–355.
4. Magnucka, E., R. Żarnowski, S. Pietr, and A. Kozubek. 2001. The influence of herbicides on biosynthesis of antifungal resorcinols by rye seedlings. *Bull. Pol. Acad. Sci.* 49:359–367.
5. 2002. Liposomal antitumor drug and its preparation, US Pat. Appl. US 20020016302A1.
6. Israelachvili, J. N., D. J. Mitchell, and B. W. Ninham. 1976. Theory of the self-assembly of hydrocarbon amphiphiles into micelles and bilayers. *J. Chem. Soc., Faraday Trans. 2*. 72:1525–1568.
7. Kozubek, A. 1995. Determination of octanol/water partition coefficients for long-chain homologs of orcinol from cereal grains. *Acta Biochim. Pol.* 42:247–252.
8. Gubernator, J., M. Stasiuk, and A. Kozubek. 1999. Dual effect of alkyl resorcinols, natural amphiphilic compounds, upon liposomal permeability. *Biochim. Biophys. Acta.* 1418:253–260.
9. Kozubek, A. 1985. Higher cardol homologues (5-alkenyl resorcinols) from rye affect the red cell membrane-water transport. *Z. Naturforsch. [C].* 40:80–84.
10. Kozubek, A. 1984. Hemolytic properties of cereal 5-*n*-alk(en)yl resorcinols. *Z. Naturforsch. [C].* 39:1132–1136.
11. Kozubek, A. 1987. The effect of 5-(*n*-alk(en)yl) resorcinols on membranes. I. Characterization of the permeability increase induced by 5-(*n*-heptadecenyl) resorcinols. *Acta Biochim. Pol.* 34:357–367.
12. Kozubek, A., and R. A. Demel. 1980. Permeability changes of erythrocytes and liposomes by 5-(*n*-alk(en)yl)resorcinols from rye. *Biochim. Biophys. Acta.* 603:220–227.
13. Przeworska, E., J. Gubernator, and A. Kozubek. 2001. Formation of liposomes by resorcinolic lipids, single-chain phenolic amphiphiles from *Anacardium occidentale L. Biochim. Biophys. Acta.* 1513:75–81.
14. Kozubek, A., A. Jezierski, and A. F. Sikorski. 1988. The effect of nonadec(en)yl resorcinol on the fluidity of liposome and erythrocyte membrane. *Biochim. Biophys. Acta.* 944:465–472.
15. Kozubek, A. 1987. The effect of 5-(*n*-alk(en)yl) resorcinols on membranes. II. Dependence on the aliphatic chain length and unsaturation. *Acta Biochim. Pol.* 34:387–394.
16. Kozubek, A., and J. Skala. 1995. Fusiogenic activity of natural amphiphiles, 5-*n*-alkyl resorcinols in a yeast protoplast system. *Z. Naturforsch. [C].* 50:656–659.
17. Kozubek, A., J. Gubernator, E. Przeworska, and M. Stasiuk. 2000. Liposomal drug delivery, the novel approach; Plarosomes. *Acta Biochim. Pol.* 47:639–649.
18. Kozubek, A., and B. Nienartowicz. 1995. Cereal grain resorcinolic lipids inhibit H_2O_2-induced peroxidation of biological membranes. *Acta Biochim. Pol.* 42:309–315.
19. Hladyszowski, J., L. Zubik, and A. Kozubek. 1998. Quantum mechanical and experimental oxidation studies of pentadecylresorcinol, olivetol, orcinol and resorcinol. *Free Radic. Res.* 28:359–368.

20. de Maria, P., P. Filipone, A. Fontana, C. Gasbarri, G. Siani, et al. 2005. Cardanol as a replacement for cholesterol into the lipid bilayer of POPC liposomes. *Colloids Surf. B Biointerfaces*. 40:11–18.

21. Kozubek, A., and R. A. Demel. 1981. The effect of 5-(*n*-alk(en)yl) resorcinols from rye on membrane structure. *Biochim. Biophys. Acta*. 642:242–251.

22. Lindahl, E., B. Hess, and D. van der Spoel. 2001. GROMACS 3.0: a package for molecular simulation and trajectory analysis. *J. Mol. Model*. 7:306–317.

23. Anézo, C., A. H. de Vries, H. D. Höltje, D. P. Tieleman, and S. J. Marrink. 2003. Methodological issues in lipid bilayer simulations. *J. Phys. Chem. B*. 107:9424–9433.

24. van Gunsteren, W.F., S.R. Billeter, A.A. Eising, P.H. Hünenberger, P. Krüger, et al. 1996. Biomolecular Simulation: The GROMOS96 Manual and User Guide. Hochschuleverlag AG an der ETH Zürich, Zürich, Switzerland.

25. Bayly, C. I., P. Cieplak, W. Cornell, and P. A. Kollman. 1993. A well-behaved electrostatic potential based method using charge restraints for deriving atomic charges: the RESP model. *J. Phys. Chem*. 97:10269–10280.

26. Berendsen, H. J. C., J. P. M. Postma, W. F. van Gunsteren, and J. Hermans. 1981. Interaction models for water in relation to protein hydration. *In* Intermolecular Forces. B. Pullman, editor. Reidel, Dordrecht, The Netherlands.

27. Hess, B., H. Bekker, H. J. C. Berendsen, and J. G. E. M. Fraaije. 1997. LINCS: a linear constraint solver for molecular simulations. *J. Comput. Chem.* 18:1463–1472.

28. Berendsen, H. J. C., J. P. M. Postma, W. F. van Gunsteren, A. DiNola, and J. R. Haak. 1984. Molecular dynamics with coupling to an external bath. *J. Chem. Phys.* 81:3684–3690.

29. Tironi, I. G., R. Sperb, P. E. Smith, and W. F. van Gunsteren. 1995. A generalized reaction field method for molecular dynamics simulations. *J. Chem. Phys*. 102:5451–5459.

30. Smith, P. E., and W. F. van Gunsteren. 1994. Consistent dielectric properties of the simple point charge and extended simple point charge water models at 277 and 300K. *J. Chem. Phys.* 100:3169–3174.

31. Siwko, M. E., S. J. Marrink, A. H. de Vries, A. Kozubek, A. J. M. Schoot-Uiterkamp, et al. 2007. Does isoprene protect plant membranes from thermal shock? A molecular dynamics study. *Biochim. Biophys. Acta*. 1768:198–206.

32. van der Spoel, D., E. Lindahl, B. Hess, G. Groenhof, A. E. Mark, et al. 2005. GROMACS: fast, flexible and free. *J. Comput. Chem*. 26:1701–1718.

33. Egberts, E., S. J. Marrink, and H. J. C. Berendsen. 1994. Molecular dynamics simulation of a phospholipid membrane. *Eur. Biophys. J*. 22:423–436.

34. de Vries, A. H., A. E. Mark, and S. J. Marrink. 2004. The binary mixing behavior of phospholipids in a bilayer: a molecular dynamics study. *J. Phys. Chem. B*. 108:2454–2463.

35. Marrink, S. J., and H. J. C. Berendsen. 1994. Simulation of water transport through a lipid membrane. *J. Phys. Chem*. 98:4155–4168.

36. Marrink, S. J., E. Lindahl, O. Edholm, and A. E. Mark. 2001. Simulation of the spontaneous aggregation of phospholipids into bilayers. *J. Am. Chem. Soc*. 123:8638–8639.

37. Hendrich, A. B., and A. Kozubek. 1991. Calorimetric study on the interactions of 5-*n*-heptadec(en)yl resorcinols from cereal grains with zwitterionic phospholipid (DPPC). *Z. Naturforsch.* [*C*]. 46:423–427.

38. Gerdon, S., S. Hoffmann, and A. Blume. 1994. Properties of mixed monolayers and bilayers of long-chain 5-*n*-alkyl resorcinols and dipalmitoylphosphatidylcholine. *Chem. Phys. Lipids*. 71:229–243.

39. Bhide, S. Y., Z. C. Zhang, and M. L. Berkowitz. 2007. Molecular dynamics simulations of SOPS and sphingomyelin bilayers containing cholesterol. *Biophys. J*. 92:1284–1295.

40. Poyry, S., T. Rog, M. Karttunen, and I. Vattulainen. 2008. Significance of cholesterol methyl groups. *J. Phys. Chem. B*. 112:2922–2929.

41. Kozubek, A., and J. H. P. Tyman. 1999. Resorcinolic lipids, the natural non-isoprenoic amphiphiles and their biological activity. *Chem. Rev.* 99:1–26.

42. Siwko, M.E. 2008. Disturb or stabilize? Effects of different molecules on biological membranes. PhD thesis, Rijksuniversiteit Groningen, The Netherlands.

43. Hoffmann, S. 1997. Structure and dynamics of long-chain 5-*n*-alkylresorcinols in phospholipid model membranes. PhD thesis, University of Kaiserslautern, Kaiserslautern, Germany.

44. Hübner, W., and A. Blume. 1998. Interactions at the lipid-water interface. *Chem. Phys. Lipids*. 96:99–123.

45. Reusch, R. N., and H. L. Sadoff. 1983. Novel lipid components of the *Azotobacter-vinelandii* CycT membrane. *Nature*. 302:268–270.

46. Leontiadou, H., A. E. Mark, and S. J. Marrink. 2006. Antimicrobial peptides in action. *J. Am. Chem. Soc*. 128:12156–12161.

47. Sengupta, D., H. Leontiadou, A. E. Mark, and S. J. Marrink. 2008. Toroidal pores formed by antimicrobial peptides show significant disorder. *Biochim. Biophys. Acta*. 1778:2308–2317.

48. Lee, H., and R. Larson. 2008. Coarse-grained molecular dynamics studies of the concentration and size dependence of fifth- and seventh-generation PAMAM dendrimers on pore formation in DMPC bilayer. *J. Phys. Chem. B*. 112:7778–7784.

49. Gurtovenko, A. A., and J. Anwar. 2007. Modulating the structure and properties of cell membranes: the molecular mechanism of action of dimethyl sulfoxide. *J. Phys. Chem. B*. 111:10453–10460.